**Advances in Nano Research**, *Vol. 7 No. 2 (2019) 99-108*
DOI: https://doi.org/10.12989/anr.2019.7.2.099


# Free vibration analysis Silicon nanowires surrounded by elastic matrix by nonlocal finite element method

Büşra Uzun [1a] and Ömer Civalek [*2]

[1] *Uludağ University, Civil Engineering Department, Bursa-Turkiye*
[2] *Akdeniz University, Civil Engineering Department, Antalya-Turkiye*

(*Received December 3, 2018, Revised March 29, 2019, Accepted April 3, 2019*)

**Abstract.** Higher-order theories are very important to investigate the mechanical properties and behaviors of nanoscale structures. In this study, a free vibration behavior of SiNW resting on elastic foundation is investigated via Eringen's nonlocal elasticity theory. Silicon Nanowire (SiNW) is modeled as simply supported both ends and clamped-free Euler-Bernoulli beam. Pasternak two-parameter elastic foundation model is used as foundation. Finite element formulation is obtained nonlocal Euler-Bernoulli beam theory. First, shape function of the Euler-Bernoulli beam is gained and then Galerkin weighted residual method is applied to the governing equations to obtain the stiffness and mass matrices including the foundation parameters and small scale parameter. Frequency values of SiNW is examined according to foundation and small scale parameters and the results are given by tables and graphs. The effects of small scale parameter, boundary conditions, foundation parameters on frequencies are investigated.

**Keywords:** nonlocal elasticity; nano beam; Euler Bernoulli beam theory; finite element formulation

## 1. Introduction

Thanks to their outstanding features like high Young modulus, low density, conductivity, flexibility, high tensile strength (Schulz *et al*. 2013, Demir and Civalek 2017, Chopra and Zettl 1998, Numanoğlu 2017) nanostructures/ nanomaterials offer a wide range of applications such as hydrogen storage, sensor, cantilever, solar cell, superconductor (Wang *et al*. 2009, Schmidt-Mende and MacManus-Driscoll 2007, Schulz *et al*. 2013). With the developing technology, the working possibilities of nano-scale structures have increased and nanotechnology has taken its place in many areas of use. It is very important to know the mechanical properties and behaviors of nanoscale devices in order to ensure a more accurate design and operation. The classical theories that are valid in the macro-scale lose their validity when the dimensions are reduced. Therefore, applying classical theories to microscale/ nanoscale structures is not give correct results. According to classical physics theories, each point of the object can be solved by the same equilibrium equations. But this does not apply to nano-scale structures. Because classical theories neglect the size effect. However, the atomic structure of the material in very small sizes becomes important and its influence cannot be ignored. Therefore, interatomic interactions should also be considered (Karlicic *et al*. 2016).

Various theories that take into account the effect of small scale such as strain gradient theory, couple stress theory, modified couple stress theory, surface elasticity theory have been studied by many researchers. Akbaş (2016) examined forced vibration analysis of simple supported viscoelastic nanobeam resting on Winkler-Pasternak elastic foundation based on modified couple stress theory. This viscoelastic nanobeam was studied with Timoshenko beam theory by using finite element method. Also, Akbaş (2018) studied static bending of an edge cracked functionally graded cantilever nanobeam subjected to transversal point load at the free end depending on modified couple stress theory by using finite element method. Ansari *et al*. (2011) investigated the free vibration of functionally graded microbeams based on the strain gradient Timoshenko beam theory. Akgöz and Civalek (2015) were studied bending analysis of non-homogenous microbeams embedded in an elastic medium via modified strain gradient elasticity theory. The elastic medium was modeled as Winkler foundation model. Asghari *et al*. (2011) developed Timoshenko beam based on the couple stress theory and they investigated size effect. Akgöz and Civalek (2013a, b) and graphene were investigated vibration response of axially functionally graded tapered Euler-Bernoulli microbeam depending on modified couple stress theory. Yaylı (2018) presented torsional vibration of restrained carbon nanotube by using modified couple stress theory. Demir *et al*. (2017) presented free vibration analysis of graphene sheet modeled thin plate on elastic medium by using modified couple stress theory. He and Lilley (2008) investigated the surface effect on the elastic behavior of the static bending NWs.

In addition these theories, nonlocal elasticity theory presented by Eringen (1983) has been extensively studied for different type (analytical and numerical) solution in

*Corresponding author, Ph.D., Professor,
E-mail: civalek@yahoo.com
[a] M.Sc. Student



ISSN: 2287-237X (Print), 2287-2388 (Online)

various analyzes such as buckling (Tounsi *et al*. 2013b, Chemi *et al*. 2015, Ebrahimi and Barati 2016, Mercan and Civalek 2016, Akgöz and Civalek 2011), vibration (Zhang *et al*. 2005, Ansari *et al*. 2010, Belkorissat *et al*. 2015, Khan and Hashemi 2016), bending (Civalek and Demir 2011, Nejad and Hadi 2016, Ansari *et al*. 2018). This theory based on the fact that the stress of a reference point depends not only on that point but also the function of the strains of all other points. Reddy (2007) presented analytical solutions of bending, vibration and buckling of various beam theories such as Euler-Bernoulli, Timoshenko, Reddy, Levinson by using nonlocal elasticity. Berrabah *et al*. (2013) were showed comparison of nonlocal Timoshenko and Reddy beam theories for bending, vibration and buckling analysis of a simply supported nanobeam. Especially carbon nanotubes have been extensively examined based on nonlocal elasticity theory (Benzair *et al*. 2008, Heireche *et al*. 2008a, b, c, Tounsi *et al*. 2008, 2013a, Rakrak *et al*. 2016).

In this study, free vibration analysis of SiNW resting on elastic foundation is investigated. The SiNW is modeled as Euler-Bernoulli beam and Pasternak foundation model with two parameters is used. Vibration characteristics related to size effect is investigated by Eringen's nonlocal elasticity theory. First, shape function of the Euler-Bernoulli beam is gained and then Galerkin weighted residual method is applied to the governing equations to obtain the stiffness and mass matrices including the foundation parameters and small scale parameter. Frequency values of SiNW is examined according to foundation and small scale parameters and the results are given by tables and graphs.

## 2. Euler Bernoulli beam theory

X, y, z point out the length, width and height of the beam and u, v, w are the displacements in the x, y, z directions, respectively. The displacements for a Bernoulli–Euler beam can be written as below (Kong *et al*. 2008)

$$u(x,z,t) = -z\frac{\partial w(x,t)}{\partial x}, \qquad v(x,z,t)=0, \qquad w(x,z,t) = w(x,t) \tag{1}$$

From Eq. (2) we find the strains of the Euler-Bernoulli beam as follows

$$\varepsilon_{ij} = \frac{1}{2}\left(\frac{\partial u_i}{\partial j} + \frac{\partial u_j}{\partial i}\right) \tag{2}$$

From Eq. (2) we find the strains of the Euler-Bernoulli beam as follows

$$\varepsilon_{xx} = \frac{1}{2}\left(\frac{\partial u(x,z,t)}{\partial x} + \frac{\partial u(x,z,t)}{\partial x}\right) = -z\frac{\partial^2 w(x,t)}{\partial x^2} \tag{3}$$

$$\varepsilon_{xz} = \varepsilon_{zx} = \frac{1}{2}\left(\frac{\partial u(x,z,t)}{\partial z} + \frac{\partial w(x,z,t)}{\partial x}\right) = \frac{1}{2}\left(-\frac{\partial w(x,t)}{\partial x} + \frac{\partial w(x,t)}{\partial x}\right) = 0 \tag{4}$$

$$\varepsilon_{xy} = \varepsilon_{yx} = \varepsilon_{yy} = \varepsilon_{yz} = \varepsilon_{zy} = \varepsilon_{zz} = 0 \tag{5}$$

All strains are zero except from $\varepsilon_{xx}$. Stress for the linear elastic materials is expressed as follows

$$\sigma = E\varepsilon \tag{6}$$

Here $\sigma$ is the stress tensor and E is the elasticity modulus of the material. $\sigma_{xx}$ is obtained if $\varepsilon_{xx}$ is written in Eq. (6) as we obtained in Eq. (3)

$$\sigma_{xx} = E\varepsilon_{xx} = -Ez\frac{\partial^2 w(x,t)}{\partial x^2} \tag{7}$$

Moment (*M*) and the moment of inertia (*I*) are given by

$$M = \int_A z\sigma_{xx} dA, \qquad I = \int_A z^2 dA \tag{8}$$

Here, A is the cross section area.

For the transverse vibration of Euler-Bernoulli beam resting on elastic foundation, the equilibrium conditions are

$$\frac{\partial V(x,t)}{\partial x} = -f(x,t) + \rho A\frac{\partial^2 w(x,t)}{\partial x^2} + k_w w(x,t) - k_g\frac{\partial^2 w(x,t)}{\partial x^2} \tag{9}$$

$$V(x,t) = \frac{\partial M(x,t)}{\partial x} \tag{10}$$

$$\frac{\partial^2 M(x,t)}{\partial x^2} = -f(x,t) + \rho A\frac{\partial^2 w(x,t)}{\partial x^2} + k_w w(x,t) - k_g\frac{\partial^2 w(x,t)}{\partial x^2} \tag{11}$$

Where $\rho$ is the mass density, $f(x,t)$ is distributed load, $k_w$ is Winkler foundation modulus and $k_g$ is Pasternak

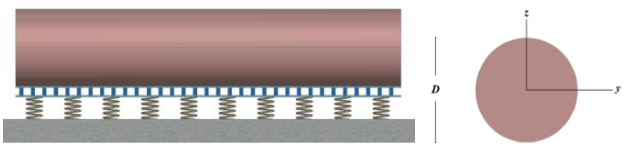


Fig. 1 Illustration of SiNW resting on elastic foundation

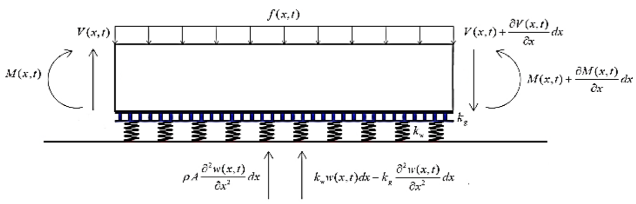


Fig. 2 Euler-Bernoulli beam resting on elastic foundation

foundation modulus. Since there is no distributed load in the beam we will analyze, $f(x,t) = 0$.

### *2.1 Nonlocal Euler Bernoulli Beam Resting on Elastic Foundation*

The nonlocal stress tensor at point x is expressed as (Eringen 1983, Yan *et al*. 2015)

$$\sigma_{ij,j} = 0 \tag{12}$$

$$\sigma_{ij}(x) = \int_V H(|x' - x|), \tau) C_{ijkl} \varepsilon_{kl} dV(x') \tag{13}$$

Where $\sigma_{ij}$ is the stress tensor, $H(|x' - x|, \tau)$ is the Kernel function, $C_{ijkl}$ is the fourth-order elastic module tensor, $\varepsilon_{kl}$ is the strain tensor, $|x' - x|$ is the distance in the Euclidean form, $\tau = \frac{e_0 a}{l}$, $e_0$ is a material constant which is determined experimentally, $a$ and $l$ are the internal and external characteristic lengths, respectively and $V$ is the region occupied by the body. The nonlocal constitutive formulation is (Reddy and Pang 2008)

$$[1 - \tau^2 l^2 \nabla^2]\sigma_{ij} = C_{ijkl}\varepsilon_{kl} \tag{14}$$

For one dimensional case, the nonlocal constitutive relations can be written as below (Eringen 1983, Phadikar and Pradhan 2010)

$$\sigma_{xx} - (e_0 a)^2 \frac{\partial^2 \sigma_{xx}}{\partial x^2} = E\varepsilon_{xx} \tag{15}$$

Multiplying z on both sides of Eq. (15) and integrating over the cross-sectional area of the beam, we obtain

$$\int_A z\sigma dA - (e_0 a)^2 \int_A z \frac{\partial^2 \sigma}{\partial x^2} dA = \int_A zE\varepsilon dA = 0 \tag{16}$$

Substituting Eqs. (3) and (8) into (16), we get

$$M(x,t) - (e_0 a)^2 \frac{\partial^2 M(x,t)}{\partial x^2} = -EI \frac{\partial^2 w(x,t)}{\partial x^2} \tag{17}$$

By differentiating Eq. (17) twice with respect to the variable x and substituting Eq. (20) into Eq. (11), we get the governing equation of vibration of Euler-Bernoulli nanobeam resting on elastic foundation

$$\begin{aligned} & EI\frac{\partial^4 w(x,t)}{\partial x^4} + \rho A \frac{\partial^2 w(x,t)}{\partial x^2} + k_w w \\ & - k_g \frac{\partial^2 w(x,t)}{\partial x^2} - (e_0 a)^2 \frac{d^2}{dx^2} \\ & \left[\rho A \frac{\partial^2 w(x,t)}{\partial x^2} + k_w w - k_g \frac{\partial^2 w(x,t)}{\partial x^2}\right] = 0 \end{aligned} \tag{18}$$

### *2.2 Shape function of beam and Galerkin weighted residual method*

The degrees of freedom of a beam element are $w_1$ (displacement of node 1), $\theta_1$ (rotation of node 1), $w_2$ (displacement of node 2), $\theta_2$ (rotation of node 2). The displacement of the beam element is expressed by four constants due to the degrees of freedom

$$\begin{aligned} w &= \alpha_0 + \alpha_1 x + \alpha_2 x^2 + \alpha_3 x^3 \\ &= [1 \quad x \quad x^2 \quad x^3] \begin{bmatrix} \alpha_0 \\ \alpha_1 \\ \alpha_2 \\ \alpha_3 \end{bmatrix} \end{aligned} \tag{19}$$

The rotation is expressed as $\theta = \frac{dw}{dx}$ and it is written from Eq. (19) as below

$$\theta = \alpha_1 + 2\alpha_2 x + 3\alpha_3 x^2 \tag{20}$$

Find the deformations of the beam element at nodes 1 (x = 0) and 2 (x = L) from Eqs. (19) and (20)

Node *1* ($x = 0$)

$$w(0) = \alpha_0 \tag{21}$$

$$\theta(0) = \alpha_1 \tag{22}$$

Node 2 ($x = L$)

$$w(L) = \alpha_0 + \alpha_1 L + \alpha_2 L^2 + \alpha_3 L^3 \tag{23}$$

$$\theta(L) = \alpha_1 + 2\alpha_2 L + 3\alpha_3 L^2 \tag{24}$$

If we write the displacement and rotation expressions in matrix form, we obtain Eq. (25)

$$\begin{Bmatrix} w_1 \\ \theta_1 \\ w_2 \\ \theta_2 \end{Bmatrix} = \begin{bmatrix} 1 & 0 & 0 & 0 \\ 0 & 1 & 0 & 0 \\ 1 & L & L^2 & L^3 \\ 0 & 1 & 2L & 3L^2 \end{bmatrix} \begin{Bmatrix} \alpha_0 \\ \alpha_1 \\ \alpha_2 \\ \alpha_3 \end{Bmatrix} \tag{25}$$

Write the coefficients $\alpha_0, \alpha_1, \alpha_2, \alpha_3$ from Eq. (25)

$$\begin{Bmatrix} \alpha_0 \\ \alpha_1 \\ \alpha_2 \\ \alpha_3 \end{Bmatrix} = \begin{bmatrix} 1 & 0 & 0 & 0 \\ 0 & 1 & 0 & 0 \\ \frac{-3}{L^2} & \frac{-2}{L} & \frac{3}{L^2} & \frac{-1}{L} \\ \frac{2}{L^3} & \frac{1}{L^2} & \frac{-2}{L^3} & \frac{1}{L^2} \end{bmatrix} \begin{Bmatrix} w_1 \\ \theta_1 \\ w_2 \\ \theta_2 \end{Bmatrix} \tag{26}$$

Substitution Eq. (26) into Eq. (19), the shape function $\varphi$ is acquired. $\xi = x/L$ is dimensionless local coordinate.

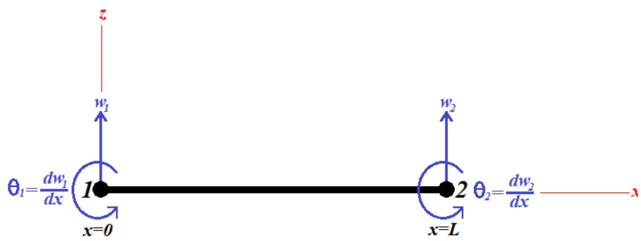


Fig. 3 Illustration of a beam element

$$\varphi = \begin{Bmatrix} \varphi_1 \\ \varphi_2 \\ \varphi_3 \\ \varphi_4 \end{Bmatrix} = \begin{Bmatrix} 1-3\xi^2+2\xi^3 \\ L(\xi-2\xi^2+\xi^3) \\ 3\xi^2-2\xi^3 \\ L(-\xi^2+\xi^3) \end{Bmatrix} \tag{27}$$

In order to get the weak form of the governing equation of nonlocal Euler-Bernoulli beam resting on elastic foundation, the residue ($I$) can be expressed as (Demir and Civalek 2017)

$$I = EI\frac{\partial^4 w(x,t)}{\partial x^4} + \rho A\frac{\partial^2 w(x,t)}{\partial x^2} + k_w w - k_g\frac{\partial^2 w(x,t)}{\partial x^2} - (e_0a)^2\frac{d^2}{dx^2}\left[\rho A\frac{\partial^2 w(x,t)}{\partial x^2} + k_w w - k_g\frac{\partial^2 w(x,t)}{\partial x^2}\right] = 0 \tag{28}$$

Eq. (28) is multiplied by a weighting function ($\varphi$) to specify the weighted residue. When the weighted residual is integrated over the length

$$\int_0^L \varphi I dx = 0 \tag{29}$$

Eq. (30) is integrated by parts. According to the chain rule, the general form

$$\int_0^L \varphi EI\frac{\partial^4 w(x,t)}{\partial x^4} + \varphi\rho A\frac{\partial^2 w(x,t)}{\partial x^2} + \varphi k_w w - \varphi k_g\frac{\partial^2 w(x,t)}{\partial x^2} - \varphi(e_0a)^2\frac{d^2}{dx^2}\left[\rho A\frac{\partial^2 w(x,t)}{\partial x^2} + k_w w - k_g\frac{\partial^2 w(x,t)}{\partial x^2}\right]dx = 0 \tag{30}$$

Eq. (30) is integrated by parts. According to the chain rule, the general form

$$\int_0^L \begin{bmatrix} EI\frac{\partial^2\varphi}{\partial x^2}\frac{\partial^2\varphi^T}{\partial x^2} + \rho A\varphi\varphi^T\ddot{w} + k_{w_{\varphi\varphi^T}} \\ -k_{g_{\frac{\partial\varphi}{\partial x}\frac{\partial\varphi^T}{\partial x}}} - (e_0a)^2\rho A\frac{\partial\varphi}{\partial x}\frac{\partial\varphi^T}{\partial x}\ddot{w} \\ -(e_0a)^2 k_{w_{\frac{\partial\varphi}{\partial x}\frac{\partial\varphi^T}{\partial x}}} k_{g_{\frac{\partial^2\varphi}{\partial x^2}\frac{\partial^2\varphi^T}{\partial x^2}}} \end{bmatrix} dx = 0 \tag{31}$$

By using the shape functions in Eq. (27) and the dimensionless local coordinate, the stiffness matrices $K^b$ (bending stiffness matrix), $K^w$ (Winkler foundation stiffness matrix), $K^g$ (shear foundation stiffness matrix) and the mass matrix $M$ are obtained

$$K^b = EI\int_0^L \begin{Bmatrix} \varphi_1'' \\ \varphi_2'' \\ \varphi_3'' \\ \varphi_4'' \end{Bmatrix}\{\varphi_1'' \quad \varphi_2'' \quad \varphi_3'' \quad \varphi_4''\}dx$$

$$= EI\int_0^L \begin{bmatrix} \varphi_1''\varphi_1'' & \varphi_1''\varphi_2'' & \varphi_1''\varphi_3'' & \varphi_1''\varphi_4'' \\ \varphi_2''\varphi_1'' & \varphi_2''\varphi_2'' & \varphi_2''\varphi_3'' & \varphi_2''\varphi_4'' \\ \varphi_3''\varphi_1'' & \varphi_3''\varphi_2'' & \varphi_3''\varphi_3'' & \varphi_3''\varphi_4'' \\ \varphi_4''\varphi_1'' & \varphi_4''\varphi_2'' & \varphi_4''\varphi_3'' & \varphi_4''\varphi_4'' \end{bmatrix}dx \tag{32}$$

$$K^b = \frac{EI}{L^3}\begin{bmatrix} 12 & 6L & -12 & 6L \\ 6L & 4L^2 & -6L & 2L^2 \\ -12 & -6L & 12 & -6L \\ 6L & 2L^2 & -6L & 4L^2 \end{bmatrix}$$

$$K^{w1} = k_w\int_0^L \begin{Bmatrix} \varphi_1 \\ \varphi_2 \\ \varphi_3 \\ \varphi_4 \end{Bmatrix}\{\varphi_1 \quad \varphi_2 \quad \varphi_3 \quad \varphi_4\}dx$$

$$= k_w\int_0^L \begin{bmatrix} \varphi_1\varphi_1 & \varphi_1\varphi_2 & \varphi_1\varphi_3 & \varphi_1\varphi_4 \\ \varphi_2\varphi_1 & \varphi_2\varphi_2 & \varphi_2\varphi_3 & \varphi_2\varphi_4 \\ \varphi_3\varphi_1 & \varphi_3\varphi_2 & \varphi_3\varphi_3 & \varphi_3\varphi_4 \\ \varphi_4\varphi_1 & \varphi_4\varphi_2 & \varphi_4\varphi_3 & \varphi_4\varphi_4 \end{bmatrix}dx \tag{33}$$

$$K^{w1} = \frac{k_w}{420}\begin{bmatrix} 156L & 22L^2 & 54L & -13L^2 \\ 22L^2 & 4L^3 & 13L^2 & -3L^3 \\ 54L & 13L^2 & 156L & -22L^2 \\ -13L^2 & -3L^3 & -22L^2 & 4L^3 \end{bmatrix}$$

$$K^{w2} = (e_0a)^2 k_w\int_0^L \begin{Bmatrix} \varphi_1' \\ \varphi_2' \\ \varphi_3' \\ \varphi_4' \end{Bmatrix}\{\varphi_1' \quad \varphi_2' \quad \varphi_3' \quad \varphi_4'\}dx$$

$$= (e_0a)^2 k_w\int_0^L \begin{bmatrix} \varphi_1'\varphi_1' & \varphi_1'\varphi_2' & \varphi_1'\varphi_3' & \varphi_1'\varphi_4' \\ \varphi_2'\varphi_1' & \varphi_2'\varphi_2' & \varphi_2'\varphi_3' & \varphi_2'\varphi_4' \\ \varphi_3'\varphi_1' & \varphi_3'\varphi_2' & \varphi_3'\varphi_3' & \varphi_3'\varphi_4' \\ \varphi_4'\varphi_1' & \varphi_4'\varphi_2' & \varphi_4'\varphi_3' & \varphi_4'\varphi_4' \end{bmatrix}dx \tag{34}$$

$$K^{w2} = \frac{(e_0a)^2 k_w}{30L}\begin{bmatrix} 36 & 3L & -36 & 3L \\ 3L & 4L^2 & -3L & -L^2 \\ -36 & -3L & 36 & -3L \\ 3L & -L^2 & -3L & 4L^2 \end{bmatrix}$$

$$K^{g1} = k_g\int_0^L \begin{Bmatrix} \varphi_1' \\ \varphi_2' \\ \varphi_3' \\ \varphi_4' \end{Bmatrix}\{\varphi_1' \quad \varphi_2' \quad \varphi_3' \quad \varphi_4'\}dx \tag{35}$$

$$= k_g \int_0^L \begin{bmatrix} \varphi_1'\varphi_1' & \varphi_1'\varphi_2' & \varphi_1'\varphi_3' & \varphi_1'\varphi_4' \\ \varphi_2'\varphi_1' & \varphi_2'\varphi_2' & \varphi_2'\varphi_3' & \varphi_2'\varphi_4' \\ \varphi_3'\varphi_1' & \varphi_3'\varphi_2' & \varphi_3'\varphi_3' & \varphi_3'\varphi_4' \\ \varphi_4'\varphi_1' & \varphi_4'\varphi_2' & \varphi_4'\varphi_3' & \varphi_4'\varphi_4' \end{bmatrix} dx$$

$$K^{g1} = \frac{k_g}{30L}\begin{bmatrix} 36 & 3L & -36 & 3L \\ 3L & 4L^2 & -3L & -L^2 \\ -36 & -3L & 36 & -3L \\ 3L & -L^2 & -3L & 4L^2 \end{bmatrix} \quad (35)$$

$$K^{g2} = (e_0a)^2 k_g \int_0^L \begin{Bmatrix} \varphi_1'' \\ \varphi_2'' \\ \varphi_3'' \\ \varphi_4'' \end{Bmatrix} \begin{Bmatrix} \varphi_1'' & \varphi_2'' & \varphi_3'' & \varphi_4'' \end{Bmatrix} dx$$

$$= (e_0a)^2 k_g \int_0^L \begin{bmatrix} \varphi_1''\varphi_1'' & \varphi_1''\varphi_2'' & \varphi_1''\varphi_3'' & \varphi_1''\varphi_4'' \\ \varphi_2''\varphi_1'' & \varphi_2''\varphi_2'' & \varphi_2''\varphi_3'' & \varphi_2''\varphi_4'' \\ \varphi_3''\varphi_1'' & \varphi_3''\varphi_2'' & \varphi_3''\varphi_3'' & \varphi_3''\varphi_4'' \\ \varphi_4''\varphi_1'' & \varphi_4''\varphi_2'' & \varphi_4''\varphi_3'' & \varphi_4''\varphi_4'' \end{bmatrix} dx \quad (36)$$

$$K^{g2} = \frac{(e_0a)^2 k_g}{L^3}\begin{bmatrix} 12 & 6L & -12 & 6L \\ 6L & 4L^2 & -6L & 2L^2 \\ -12 & -6L & 12 & -6L \\ 6L & 2L^2 & -6L & 4L^2 \end{bmatrix}$$

$$M^1 = \rho A \int_0^L \begin{Bmatrix} \varphi_1 \\ \varphi_2 \\ \varphi_3 \\ \varphi_4 \end{Bmatrix} \begin{Bmatrix} \varphi_1 & \varphi_2 & \varphi_3 & \varphi_4 \end{Bmatrix} dx$$

$$= \rho A \int_0^L \begin{bmatrix} \varphi_1\varphi_1 & \varphi_1\varphi_2 & \varphi_1\varphi_3 & \varphi_1\varphi_4 \\ \varphi_2\varphi_1 & \varphi_2\varphi_2 & \varphi_2\varphi_3 & \varphi_2\varphi_4 \\ \varphi_3\varphi_1 & \varphi_3\varphi_2 & \varphi_3\varphi_3 & \varphi_3\varphi_4 \\ \varphi_4\varphi_1 & \varphi_4\varphi_2 & \varphi_4\varphi_3 & \varphi_4\varphi_4 \end{bmatrix} dx \quad (37)$$

$$M^1 = \frac{\rho A}{420}\begin{bmatrix} 156L & 22L & 54L & -13L^2 \\ 22L^2 & 4L^3 & 13L^2 & -3L^3 \\ 54L & 13L^2 & 156L & -22L^2 \\ -13L^2 & -3L^3 & -22L^2 & 4L^3 \end{bmatrix}$$

$$M^2 = (e_0a)^2 \rho A \int_0^L \begin{Bmatrix} \varphi_1' \\ \varphi_2' \\ \varphi_3' \\ \varphi_4' \end{Bmatrix} \begin{Bmatrix} \varphi_1' & \varphi_2' & \varphi_3' & \varphi_4' \end{Bmatrix} dx$$

$$= (e_0a)^2 \rho A \int_0^L \begin{bmatrix} \varphi_1'\varphi_1' & \varphi_1'\varphi_2' & \varphi_1'\varphi_3' & \varphi_1'\varphi_4' \\ \varphi_2'\varphi_1' & \varphi_2'\varphi_2' & \varphi_2'\varphi_3' & \varphi_2'\varphi_4' \\ \varphi_3'\varphi_1' & \varphi_3'\varphi_2' & \varphi_3'\varphi_3' & \varphi_3'\varphi_4' \\ \varphi_4'\varphi_1' & \varphi_4'\varphi_2' & \varphi_4'\varphi_3' & \varphi_4'\varphi_4' \end{bmatrix} dx \quad (38)$$

Table 1 Comparison of first three non-dimensional frequencies for various $e_0a/L$ with S-S and C-F boundary conditions

| | | S-S | | | C-F | | |
|---|---|---|---|---|---|---|---|
| | | $\varpi_1$ | $\varpi_2$ | $\varpi_3$ | $\varpi_1$ | $\varpi_2$ | $\varpi_3$ |
| **$e_0a/L$** | **Analytical** | **9.8696** | **39.4784** | **88.8264** | **3.5160** | **22.0345** | **61.6972** |
| **0** | **N** | | | | | | |
| | **4** | 9.8722 | 39.6342 | 90.4495 | 3.5161 | 22.0602 | 62.1749 |
| | **5** | 9.8707 | 39.5438 | 89.5319 | 3.5161 | 22.0455 | 61.9188 |
| | **6** | 9.8701 | 39.5104 | 89.1770 | 3.5160 | 22.0399 | 61.8101 |
| | **7** | 9.8699 | 39.4958 | 89.0191 | 3.5160 | 22.0375 | 61.7600 |
| | **8** | 9.8698 | 39.4887 | 88.9407 | 3.5160 | 22.0363 | 61.7347 |
| **$e_0a/L$** | **Analytical** | **8.3569** | **24.5823** | **41.6285** | **3.2258** | **14.5756** | **31.3808** |
| **0.2** | **N** | | | | | | |
| | **4** | 8.3591 | 24.6765 | 42.3335 | 3.2259 | 14.5856 | 31.5763 |
| | **5** | 8.3578 | 24.6222 | 41.9422 | 3.2258 | 14.5798 | 31.4684 |
| | **6** | 8.3574 | 24.6019 | 41.7866 | 3.2258 | 14.5777 | 31.4249 |
| | **7** | 8.3572 | 24.5930 | 41.7162 | 3.2258 | 14.5767 | 31.4052 |
| | **8** | 8.3571 | 24.5886 | 41.6808 | 3.2258 | 14.5762 | 31.3954 |
| **$e_0a/L$** | **Analytical** | **6.1456** | **14.5951** | **22.7743** | **2.6447** | **9.2336** | **18.1027** |
| **0.4** | **N** | | | | | | |
| | **4** | 6.1472 | 14.6503 | 23.1534 | 2.6447 | 9.2407 | 18.2336 |
| | **5** | 6.1462 | 14.6186 | 22.9441 | 2.6447 | 9.2366 | 18.1606 |
| | **6** | 6.1459 | 14.6067 | 22.8601 | 2.6447 | 9.2350 | 18.1317 |
| | **7** | 6.1457 | 14.6014 | 22.8220 | 2.6447 | 9.2344 | 18.1188 |
| | **8** | 6.1457 | 14.5988 | 22.8028 | 2.6447 | 9.2340 | 18.1123 |

$$M^2 = \frac{(e_0 a)^2 \rho A}{30L} \begin{bmatrix} 36 & 3L & -36 & 3L \\ 3L & 4L^2 & -3L & -L^2 \\ -36 & -3L & 36 & -3L \\ 3L & -L^2 & -3L & 4L^2 \end{bmatrix} \quad (38)$$

The vibration of the Euler-Bernoulli beam is found as follows

$$\left| K - \omega^2 M \right| = 0 \quad (39)$$

Table 2 Comparison of first three non-dimensional frequencies errors for various $e_0a/L$ with N

| $e_0a/L$ | Mode numbers | Analytical | N = 5 | Error (%) | N = 20 | Error (%) | N = 50 | Error (%) |
|---|---|---|---|---|---|---|---|---|
| 0 | 1 | 12.1143 | 12.1152 | 0.0074 | 12.1143 | 0.0000 | 12.1143 | 0.0000 |
| | 2 | 41.9039 | 41.9658 | 0.1477 | 41.9042 | 0.0007 | 41.9039 | 0.0000 |
| | 3 | 91.2922 | 91.9811 | 0.7546 | 91.2952 | 0.0033 | 91.2923 | 0.0001 |
| 0.1 | 1 | 11.7476 | 11.7485 | 0.0077 | 11.7476 | 0.0000 | 11.7476 | 0.0000 |
| | 2 | 36.2602 | 36.3135 | 0.1470 | 36.2604 | 0.0006 | 36.2602 | 0.0000 |
| | 3 | 67.99 | 68.4880 | 0.7325 | 67.9922 | 0.0032 | 67.9901 | 0.0001 |
| 0.2 | 1 | 10.9172 | 10.9181 | 0.0082 | 10.9172 | 0.0000 | 10.9172 | 0.0000 |
| | 2 | 28.314 | 28.3556 | 0.1469 | 28.3142 | 0.0007 | 28.3140 | 0.0000 |
| | 3 | 46.659 | 46.9952 | 0.7205 | 46.6605 | 0.0032 | 46.6591 | 0.0002 |
| 0.3 | 1 | 10.0466 | 10.0474 | 0.0080 | 10.0466 | 0.0000 | 10.0466 | 0.0000 |
| | 2 | 23.2314 | 23.2659 | 0.1485 | 23.2316 | 0.0009 | 23.2314 | 0.0000 |
| | 3 | 36.3505 | 36.6123 | 0.7202 | 36.3517 | 0.0033 | 36.3506 | 0.0003 |
| 0.4 | 1 | 9.3336 | 9.3344 | 0.0086 | 9.3336 | 0.0000 | 9.3336 | 0.0000 |
| | 2 | 20.2585 | 20.2890 | 0.1506 | 20.2587 | 0.0010 | 20.2585 | 0.0000 |
| | 3 | 31.0291 | 31.2534 | 0.7229 | 31.0301 | 0.0032 | 31.0291 | 0.0000 |

Table 3 First five non-dimensional frequencies for various Winkler and Pasternak parameters with S-S and C-F boundary conditions

| KW | KG | Boundary conditions | $\varpi_1$ | $\varpi_2$ | $\varpi_3$ | $\varpi_4$ | $\varpi_5$ |
|---|---|---|---|---|---|---|---|
| 0 | 0 | S-S | 9.4159 | 33.4277 | 64.6414 | 98.3292 | 132.5067 |
| | | C-F | 3.4368 | 19.1364 | 46.4936 | 78.2131 | 111.8128 |
| 0 | 5 | S-S | 11.7476 | 36.2602 | 67.9900 | 102.2654 | 137.0829 |
| | | C-F | 5.7191 | 22.5255 | 49.8177 | 81.8857 | 116.0170 |
| 5 | 0 | S-S | 9.6777 | 33.5024 | 64.6801 | 98.3546 | 132.5256 |
| | | C-F | 4.1002 | 19.2666 | 46.5473 | 78.2451 | 111.8352 |
| 5 | 5 | S-S | 11.9585 | 36.3291 | 68.0268 | 102.2898 | 137.1012 |
| | | C-F | 6.1406 | 22.6362 | 49.8679 | 81.9163 | 116.0386 |
| 10 | 50 | S-S | 24.3339 | 55.6896 | 92.8969 | 132.5682 | 172.9307 |
| | | C-F | 13.8122 | 41.6575 | 73.5551 | 109.7086 | 148.6756 |
| 50 | 10 | S-S | 15.4063 | 39.5246 | 71.5317 | 106.2910 | 141.6878 |
| | | C-F | 10.0614 | 26.4090 | 53.4199 | 85.6985 | 120.2839 |
| 25 | 25 | S-S | 18.9842 | 46.1451 | 80.1509 | 116.7967 | 154.1153 |
| | | C-F | 11.2572 | 32.9216 | 61.6436 | 95.3434 | 131.6058 |
| 0 | 100 | S-S | 32.7966 | 71.1706 | 114.2854 | 159.5619 | 205.5044 |
| | | C-F | 18.2899 | 55.0352 | 93.0213 | 134.0218 | 178.0504 |
| 100 | 0 | S-S | 13.7353 | 34.8914 | 65.4103 | 98.8364 | 132.8835 |
| | | C-F | 10.5741 | 21.5917 | 47.5568 | 78.8498 | 112.2591 |
| 100 | 100 | S-S | 34.2873 | 71.8697 | 114.7221 | 159.8750 | 205.7476 |
| | | C-F | 20.8452 | 55.9363 | 93.5573 | 134.3943 | 178.3310 |

Table 4 First five non-dimensional frequencies for various Winkler and Pasternak parameters and $e_0a$

| | | KW = 0 & KG = 0 | | KW = 10 & KG = 10 | |
|---|---|---|---|---|---|
| **$e_0$a** | **$\varpi_n$** | **S-S** | **C-F** | **S-S** | **C-F** |
| | 1 | 9.8696 | 3.5160 | 14.3564 | 7.8341 |
| | 2 | 39.4784 | 22.0345 | 44.3095 | 28.4705 |
| 0 | 3 | 88.8264 | 61.6972 | 93.7465 | 67.7321 |
| | 4 | 157.9137 | 120.9019 | 162.8677 | 126.7095 |
| | 5 | 246.7402 | 199.8596 | 251.7104 | 205.5107 |
| | 1 | 9.8688 | 3.5159 | 14.3558 | 7.8341 |
| | 2 | 39.4660 | 22.0288 | 44.2984 | 28.4650 |
| 1 | 3 | 88.7634 | 61.6591 | 93.6867 | 67.6951 |
| | 4 | 157.7146 | 120.7639 | 162.6746 | 126.5744 |
| | 5 | 246.2546 | 199.4958 | 251.2344 | 205.1525 |
| | 1 | 9.8665 | 3.5155 | 14.3542 | 7.8340 |
| | 2 | 39.4286 | 22.0117 | 44.2651 | 28.4486 |
| 2 | 3 | 88.5750 | 61.5452 | 93.5083 | 67.5845 |
| | 4 | 157.1217 | 120.3528 | 162.0999 | 126.1720 |
| | 5 | 244.8148 | 198.4163 | 249.8233 | 204.0894 |

Table 5 First five non-dimensional frequencies for various Winkler and Pasternak parameters and $e_0a$

| | | KW = 25 & KG = 25 | | KW = 50 & KG = 50 | |
|---|---|---|---|---|---|
| **$e_0$a** | **$\varpi_n$** | **S-S** | **C-F** | **S-S** | **C-F** |
| | 1 | 19.2133 | 11.1471 | 25.3158 | 14.8998 |
| | 2 | 50.7002 | 35.5740 | 59.8537 | 44.3882 |
| 0 | 3 | 100.6767 | 75.7925 | 111.2720 | 87.3085 |
| | 4 | 170.0282 | 134.9240 | 181.3351 | 147.4901 |
| | 5 | 258.9869 | 213.6973 | 270.6801 | 226.6405 |
| | 1 | 19.2129 | 11.1473 | 25.3155 | 14.9003 |
| | 2 | 50.6905 | 35.5691 | 59.8455 | 44.3846 |
| 1 | 3 | 100.6211 | 75.7572 | 111.2217 | 87.2759 |
| | 4 | 169.8433 | 134.7930 | 181.1617 | 147.3654 |
| | 5 | 258.5243 | 213.3469 | 270.2376 | 226.3021 |
| | 1 | 19.2117 | 11.1479 | 25.3146 | 14.9020 |
| | 2 | 50.6614 | 35.5545 | 59.8209 | 44.3735 |
| 2 | 3 | 100.4550 | 75.6515 | 111.0714 | 87.1784 |
| | 4 | 169.2929 | 134.4027 | 180.6458 | 146.9936 |
| | 5 | 257.1532 | 212.3070 | 268.9262 | 225.2977 |

## 3. Numerical results

In this section, the frequency values of SiNW are obtained with various aspect radios (L/D), various non-dimensional small scale parameters (e0a/L), different dimensionless Winkler and Pasternak parameters (KW and KG), different boundary conditions and different number of elements (N). Boundary conditions are simply supported at both ends (S–S) and clamped-free (C–F). The results obtained are shown in tables and graphs. The dimensionless Winkler parameter, the dimensionless Pasternak parameter and the dimensionless frequency expressed in the formulas below, are used for the results in the tables

$$KW = \frac{k_w L^4}{EI}, \quad KG = \frac{k_g L^4}{EI}, \quad \varpi = \omega L^2 \sqrt{\frac{\rho A}{EI}} \tag{4}$$

Table 1 shows the non-dimensional frequency values of the different $e_0a/L$ values of a nanowire with S-S and C-F boundary conditions. Both analytical and finite element solutions are compared with the results. As the number of elements N increase, the results close to the analytical solution. It is also seen that the frequency decreases with increasing $e_0a/L$ value.

In Table 2, the frequency values of the first three modes at different $e_0a/L$ values are given by analytical and finite element solution. According to the table, by increasing the mode numbers, the error percentage increases and by increasing element number N, the error percentage decreases. In the following table (Table 3), the dimensionless frequencies of the nanowire with S-S and C-F boundary conditions in the different Winkler and Pasternak parameter values are given in the first 5 modes. Frequency values increase as KW and KG values increase.

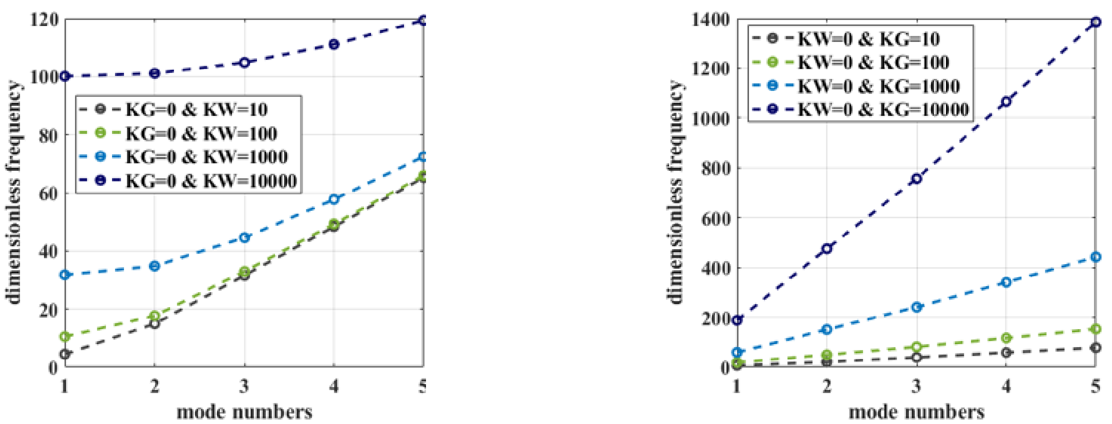


(a) KG = 0 (b) KW = 0

Fig. 6 Variation of dimensionless frequency values with different KW and KG values

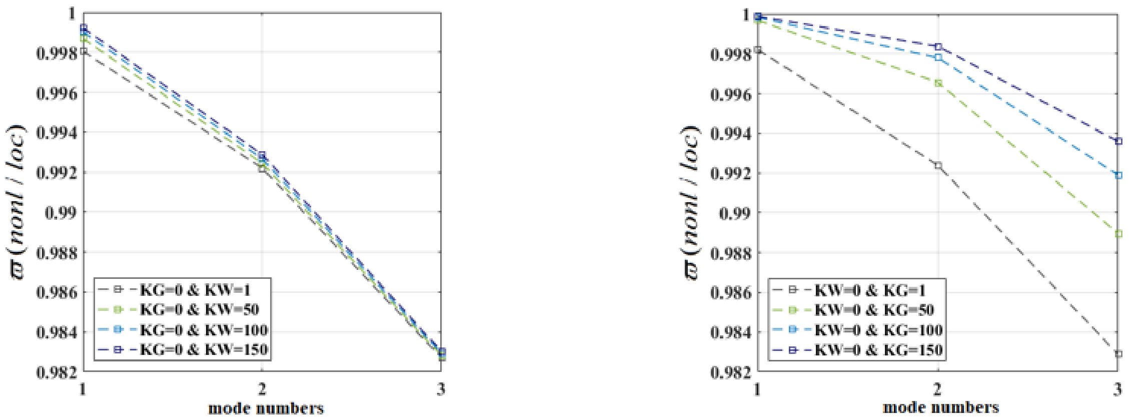


(a) KG = 0 (b) KW = 0

Fig. 7 Variation of dimensionless nonlocal / local frequency ratios with different KW and KG values

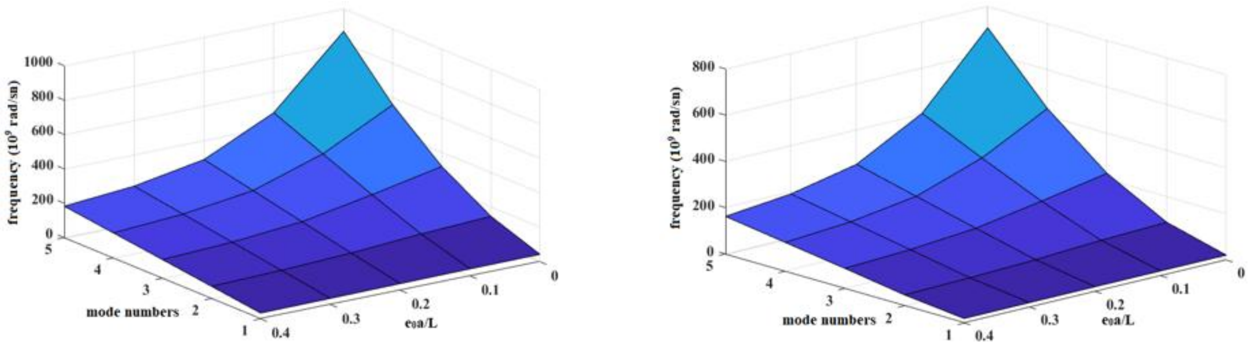


(a) S-S (b) C-F

Fig. 8 Variation of frequency values with non-dimensional small scale parameter and mode numbers

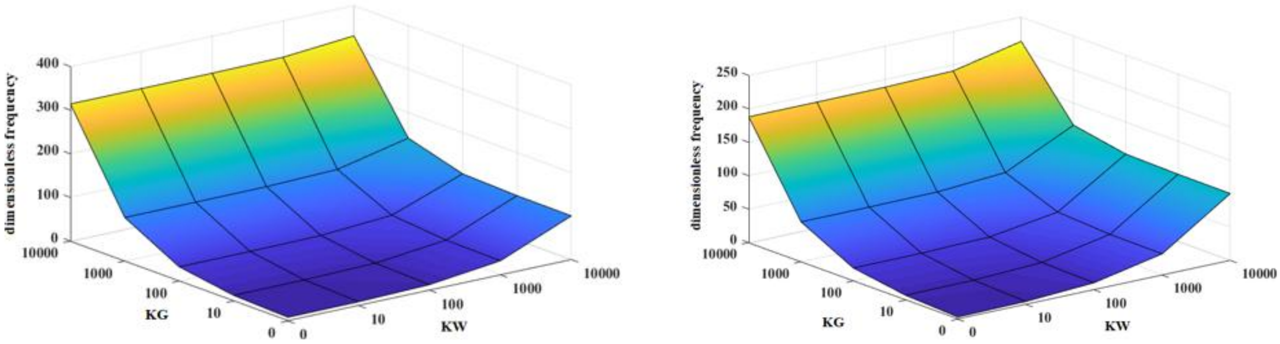


(a) S-S (b) C-F

Fig. 9 Variation of dimensionless frequency values with KW and KG

As can be seen from the results, the effect of KG on the frequency value is much greater than the effect of KW.

For KW = 0, KG = 0 and KW = 10, KG = 10 values, at first five modes dimensionless frequencies are given in Table 4. For KW = 25, KG = 25 and KW = 100, KG = 100 values, at first five modes dimensionless frequencies are given in Table 5. In Table 4, the frequencies of the nanowire with both boundary conditions decrease with increasing e0a values. When looking at Table 5, a different situation is seen. The frequency values of the S-S boundary condition in each mode are reduced with increasing e0a, but the frequencies of the C-F boundary condition in the first mode increase with increasing e0a, while the frequencies in other modes decrease.

## 4. Conclusions

In this paper, free vibration analysis of SiNW is investigated based on the Nonlocal Euler-Bernoulli beam theory. Solutions are obtained for S-S and C-F boundary conditions. According to the obtained results

- As the number of elements N increase, the results close to the analytical solution.
- Frequency decreases with increasing e0a/L value.
- By increasing the mode numbers, the error percentage increases.
- By increasing element number N, the error percentage decreases.
- The frequency values of C-F smaller than S-S.
- Frequency values increase as KW and KG values increase. The effect of KG on the frequency values is much greater than the effect of KW.
- Frequencies of S-S beam in each mode for each KW and KG value decrease, by increasing e0a.
- Frequencies except from first mode of C-F beam for each KW and KG value decrease, by increasing e0a. But when KW and KG exceed a value (in table 5 KW = KG = 25), frequencies of first mode increase by increasing e0a)
- As L/D ratio increase, frequencies decrease.

## Acknowledgments

This study has been supported by The Scientific and Technological Research Council of Turkey (TÜBİTAK) with Project no: 117M495. This support is gratefully acknowledged.

## References

Akbaş, Ş.D. (2016), "Forced vibration analysis of viscoelastic nanobeams embedded in an elastic medium", *Smart Struct. Syst., Int. J.*, **18**(6), 1125-1143.

Akbas, S.D. (2018), "Bending of a cracked functionally graded nanobeam", *Adv. Nano Res., Int. J.*, **6**(3), 219-242.

Akgöz, B. and Civalek, O. (2011), "Buckling analysis of cantilever carbon nanotubes using the strain gradient elasticity and modified couple stress theories", *J. Computat. Theor. Nanosci.*, **8**, 1821-1827.

Akgöz, B. and Civalek, Ö. (2013a), "Free vibration analysis of axially functionally graded tapered Bernoulli–Euler microbeams based on the modified couple stress theory", *Compos. Struct.*, **98**, 314-322.

Akgöz, B. and Civalek, Ö. (2013b), "Vibration analysis of micro-scaled sector shaped graphene surrounded by an elastic matrix", *Computat. Mater. Sci.*, **77**, 295-303.

Akgöz, B. and Civalek, Ö. (2015), "Bending analysis of FG microbeams resting on Winkler elastic foundation via strain gradient elasticity", *Compos. Struct.*, **134**, 294-301.

Ansari, R., Rajabiehfard, R. and Arash, B. (2010), "Nonlocal finite element model for vibrations of embedded multi-layered graphene sheets", *Computat. Mater. Sci.*, **49**(4), 831-838.

Ansari, R., Gholami, R. and Sahmani, S. (2011), "Free vibration analysis of size-dependent functionally graded microbeams based on the strain gradient Timoshenko beam theory", *Compos. Struct.*, **94**(1), 221-228.

Ansari, R., Torabi, J. and Norouzzadeh, A. (2018), "Bending analysis of embedded nanoplates based on the integral formulation of Eringen's nonlocal theory using the finite element method", *Physica B: Condensed Matter*, **534**, 90-97.

Asghari, M., Kahrobaiyan, M.H., Rahaeifard, M. and Ahmadian, M.T. (2011), "Investigation of the size effects in Timoshenko beams based on the couple stress theory", *Arch. Appl. Mech.*, **81**(7), 863-874

Belkorissat, I., Houari, M.S.A., Tounsi, A., Bedia, E.A. and Mahmoud, S.R. (2015), "On vibration properties of functionally graded nano-plate using a new nonlocal refined four variable model", *Steel Compos. Struct., Int. J.*, **18**(4), 1063-1081.

Benzair, A., Tounsi, A., Besseghier, A., Heireche, H., Moulay, N. and Boumia, L. (2008), "The thermal effect on vibration of single-walled carbon nanotubes using nonlocal Timoshenko beam theory", *J. Phys. D: Appl. Phys.*, **41**(22), 225404.

Berrabah, H.M., Tounsi, A., Semmah, A. and Adda, B. (2013), "Comparison of various refined nonlocal beam theories for bending, vibration and buckling analysis of nanobeams", *Struct. Eng. Mech., Int. J.*, **48**(3), 351-365.

Chemi, A., Heireche, H., Zidour, M., Rakrak, K. and Bousahla, A.A. (2015), "Critical buckling load of chiral double-walled carbon nanotube using non-local theory elasticity", *Adv. Nano Res., Int. J.*, **3**(4), 193-206

Chopra, N.G. and Zettl, A. (1998), "Measurement of the elastic modulus of a multi-wall boron nitride nanotube", *Solid State Commun.*, **105**(5), pp. 297-300.

Civalek, Ö. and Demir, Ç. (2011), "Bending analysis of microtubules using nonlocal Euler–Bernoulli beam theory", *Appl. Math. Model.*, **35**(5), 2053-2067.

Demir, Ç. and Civalek, Ö. (2017), "A new nonlocal FEM via Hermitian cubic shape functions for thermal vibration of nano beams surrounded by an elastic matrix", *Compos. Struct.*, **168**, 872-884.

Demir, Ç., Akgöz, B., Erdinç, M.C., Mercan, K. and Civalek, Ö. (2017), "Elastik bir ortamdaki grafen tabakanın titreşim hesabı", *Gazi Üniversitesi Mühendislik-Mimarlık Fakültesi Dergisi*, **32**(2).

Ebrahimi, F. and Barati, M.R. (2016), "An exact solution for buckling analysis of embedded piezoelectro-magnetically actuated nanoscale beams", *Adv. Nano Res., Int. J.*, **4**(2), 65-84.

Eringen, A.C. (1983), "On differential equations of nonlocal elasticity and solutions of screw dislocation and surface waves", *J. Appl. Phys.*, **54**(9), pp. 4703-4710.

He, J. and Lilley, C.M. (2008), "Surface stress effect on bending resonance of nanowires with different boundary conditions", *Appl. Phys. Lett.*, **93**(26), 263108.

Heireche, H., Tounsi, A., Benzair, A., Maachou, M. and Bedia, E.A. (2008a), "Sound wave propagation in single-walled carbon nanotubes using nonlocal elasticity", *Physica E: Low-dimens. Syst. Nanostruct.*, **40**(8), 2791-2799.

Heireche, H., Tounsi, A. and Benzair, A. (2008b), "Scale effect on wave propagation of double-walled carbon nanotubes with initial axial loading", *Nanotechnology*, **19**(18), 185703.

Heireche, H., Tounsi, A., Benzair, A. and Mechab, I. (2008c), "Sound wave propagation in single Carbon nanotubes with initial axial stress", *J Appl. Phys.*, **104**, 014301.

Karlicic, D., Murmu, T., Adhikari, S. and McCarthy, M. (2016), *Non-local Structural Mechanics*, John Wiley & Sons.

Khan, I.A. and Hashemi, S.M. (2016), "On Finite Element Vibration Analysis of Carbon Nanotubes", In: *Perusal of the Finite Element Method, InTech*, pp. 69-88.

Kong, S., Zhou, S., Nie, Z. and Wang, K. (2008), "The size-dependent natural frequency of Bernoulli–Euler micro-beams", *Int. J. Eng. Sci.*, **46**(5), 427-437.

Mercan, K. and Civalek, O. (2016), "DSC method for buckling analysis of boron nitride nanotube (BNNT) surrounded by an elastic matrix", *Compos. Struct.*, **143**, 300-309.

Nejad, M.Z. and Hadi, A. (2016), "Eringen's non-local elasticity theory for bending analysis of bi-directional functionally graded Euler–Bernoulli nano-beams", *Int. J. Eng. Sci.*, **106**, 1-9.

Numanoğlu, H.M. (2017), Nanoyapıların Kiriş ve Çubuk Modellerinin Yerel Olmayan Elastisite Teorisi Kullanılarak Titreşim Analizi, Lisans Tezi, Akdeniz Üniversitesi.

Phadikar, J.K. and Pradhan, S.C. (2010), “Variational formulation and finite element analysis for nonlocal elastic nanobeams and nanoplates”, *Computat. Mater. Sci.*, **49**(3), 492-499.

Rakrak, K., Zidour, M., Heireche, H., Bousahla, A.A. and Chemi, A. (2016), “Free vibration analysis of chiral double-walled carbon nanotube using non-local elasticity theory”, *Adv. Nano Res., Int. J.*, **4**(1), 31-44.

Reddy, J.N. (2007), “Nonlocal theories for bending, buckling and vibration of beams”, *Int. J. Eng. Sci.*, **45**(2-8), 288-307.

Reddy, J.N. and Pang, S.D. (2008), “Nonlocal continuum theories of beams for the analysis of carbon nanotubes”, *J. Appl. Phys.*, **103**(2), 023511.

Schmidt-Mende, L. and MacManus-Driscoll, J.L. (2007), “ZnO–nanostructures, defects, and devices”, *Materials Today*, **10**(5), 40-48.

Schulz, M., Shanov, V. and Yin, Z. (Eds.) (2013), *Nanotube superfiber materials: changing engineering design*, William Andrew.

Tounsi, A., Heireche, H., Berrabah, H.M., Benzair, A. and Boumia, L. (2008), “Effect of small size on wave propagation in double-walled carbon nanotubes under temperature field”, *J. Appl. Phys.*, **104**(10), 104301.

Tounsi, A., Benguediab, S., Adda, B., Semmah, A. and Zidour, M. (2013a), “Nonlocal effects on thermal buckling properties of double-walled carbon nanotubes”, *Adv. Nano Res., Int. J.*, **1**(1), 1-11.

Tounsi, A., Semmah, A. and Bousahla, A.A. (2013b), “Thermal buckling behavior of nanobeam using an efficient higher-order nonlocal beam theory”, *J. Nanomech. Micromech.* (ASCE), **3**(3), 37-42.

Wang, J., Lee, C.H., Bando, Y., Golberg, D. and Yap, Y.K. (2009), “Multiwalled boron nitride nanotubes: growth, properties, and applications”, In: *BCN Nanotubes and Related Nanostructures*, Springer, New York, NY, USA, pp. 23-44.

Yan, J.W., Tong, L.H., Li, C., Zhu, Y. and Wang, Z.W. (2015), “Exact solutions of bending deflections for nano-beams and nano-plates based on nonlocal elasticity theory”, *Compos. Struct.*, **125**, 304-313.

Yaylı, M.Ö. (2018), “Torsional vibrations of restrained nanotubes using modified couple stress theory”, *Microsyst. Technol.*, 1-11.

Zhang, Y.Q., Liu, G.R. and Xie, X.Y. (2005), “Free transverse vibrations of double-walled carbon nanotubes using a theory of nonlocal elasticity”, *Phys. Rev. B*, **71**(19), 195404.

*CC*